J Mater Sci (2011) 46:2370–2378
DOI 10.1007/s10853-010-5084-1

Microstructure modification of Al–17%Si alloy by addition of Mg

Alireza Hekmat-Ardakan · Frank Ajersch · X.-Grant Chen

Received: 27 August 2010 / Accepted: 12 November 2010 / Published online: 30 November 2010
© Springer Science+Business Media, LLC 2010

Abstract The calculated phase diagrams of Al–17%Si alloy with additions of Mg up to 10 wt% Mg have indicated two critical compositions at 4.6 and 6.8% Mg where the liquidus, the binary reaction temperatures as well as the temperature range of the formation of Mg_2Si particles are changed. The eutectic formation temperature is decreased with the addition of Mg up to 4.6% Mg, followed by constant value due to the change of the eutectic formation reaction from the binary (Liq. → Al ± Si) to the ternary (Liq. → Al + Si + Mg_2Si) reaction. This change contributes to the transformation of the eutectic silicon in matrix from long platelet, to fine and compact particles resulting in overall increased hardness of the high Mg alloys even though the hardness of the primary Mg_2Si particles is much smaller than that of the primary silicon particles. A pronounced decrease of both primary and eutectic silicon particles size was also observed for 0.4% Mg alloy when compared to the base alloy showing significant microstructural modification.

Introduction

Hypereutectic aluminum–silicon (Al–Si) alloys are widely used in the automotive, aerospace, and military industries for the applications that require low density, high specific elasticity modulus, high strength, good wear resistance, low thermal expansion coefficient, and high thermal conductivity [1–3]. Their excellent wear resistance is provided by the presence of the primary Si phase dispersed in the eutectic network of Al + Si phase. However, the high latent heat and consequent long solidification time of these alloys during conventional casting results in the precipitation of coarse Si particles, either in the form of eutectic or primary phases and adversely affect the mechanical properties, which strongly depend on the size, shape, and distribution of Si phases [4, 5]. Many studies have been carried out the modification of Si particles by using either different alloy structure modifiers [6, 7], such as rare earth (RE) elements or by using different casting processes such as rheo-casting [8], thixo-forming [9], spray deposition [10], or cooling slope casting [11].

The present study investigates the modification of the microstructure of conventionally cast non-commercial binary hypereutectic Al–Si alloy with the addition of Mg. It was previously shown by the authors [12, 13] as well as by Mandal et al. [14] that the presence of the Mg in commercial A390 alloy (Al–17%Si–4.5%Cu–0.5%Mg) changes the morphology of both the eutectic phase and the Si particles, forming intermetallic particles of Mg_2Si which appear as both eutectic and primary phases in the microstructure. However, it was found interesting to study the effect of Mg on non-commercial binary Al–17%Si in the absence of the 4.5% Cu. There are many similarities between Mg_2Si and Si particles in terms of properties and solidification behavior [15]. Both phases have a high melting temperature, low density, high hardness, and low thermal expansion coefficient. According to the calculations, the microstructure of the binary Al–17%Si alloy with minimum 11% Mg contains the particles of only primary Mg_2Si intermetallics dispersed in the eutectic matrix while

A. Hekmat-Ardakan (✉) · F. Ajersch
Dép. de Génie Chimique, École Polytechnique de Montréal, P.O. Box 6079, Centre-ville, Montreal, QC H3C 3A7, Canada
e-mail: alireza.hekmat-ardakan@polymtl.ca

X.-G. Chen
Dép. des sciences appliquées, Université du Québec à Chicoutimi (UQAC), 555, boulevard de l'Université, Chicoutimi, QC G7H 2B1, Canada

a mixture of Mg_2Si and Si particles are observed in the microstructure of the alloy with <11% Mg. The most important advantage is the possibility of producing lighter components due to the lower density of Mg_2Si (1.99 g cm^{-3}) compared to Si (2.33 g cm^{-3}), which can contribute to the light weighting of the vehicles [16], as well as providing excellent wear resistance [17].

The phase diagram of Al–17%Si alloy with additions of up to 10% Mg is investigated in the present study in order to better understand the solidification behavior and compound formation of these alloys. The thermodynamic investigation was carried out using the FactSage® software developed by the CRCT group at *Ecole Polytechnique de Montreal* using the FSlite (FactSage light metal alloy database) database. The FactSage's FSlite light alloy database was complied from the European COST Action 507 (COST 507, Thermochemical database for light metal alloys) [18]. The results of thermodynamic calculations are presented for equilibrium conditions and all compositions and solid fractions are given in weight percent (wt%). To confirm the computed results and to study the impact of Mg on the microstructure evolution of Al–17%Si, several alloys with different Mg levels were conventionally cast and thermal analysis during solidification was carried out.

Experiment

Table 1 shows the chemical compositions of test alloys used in this work. The binary Al–17%Si as the base alloy as well as alloys with 0.4, 3, 6 and 10% Mg were prepared by melting proportional amounts of commercial pure aluminum ingot (99.7%), Al-50%Si master alloy and commercial pure magnesium (99.8%).

In each test, approximately 3 kg of material was melted in a clay–graphite crucible using an electric resistance furnace. The melt temperature was maintained at ~750 °C for 30 min. Approximately 150 g of liquid metal was then poured into a preheated, thin shell crucible made of stainless steel. All alloys were cast at temperatures between 700 and 710 °C. During the cooling, two K-type thermocouples were positioned in both the center and the near-wall regions of the crucible to measure the temperature. The temperature–time data was recorded by a data acquisition system with 0.1 s scan rate. All cast samples was cooled in the static air resulting in a slow cooling rate of about 0.2 K/s.

Table 1 The chemical compositions of the test alloys

Test alloys	Al	Si	Cu	Mg	Fe	Mn	Zn	P	Ti
Base alloy	Bal.	17.31	0.00	0.08	0.15	0.01	0.003	0.00	0.01
0.4% Mg	Bal.	16.83	0.00	0.39	0.13	0.01	0.003	0.0003	0.01
3% Mg	Bal.	17.14	0.00	2.79	0.14	0.01	0.004	0.0001	0.01
6% Mg	Bal.	16.53	0.00	6.48	0.13	0.01	0.002	0.0002	0.01
10% Mg	Bal.	16.29	0.00	10.25	0.14	0.01	0.003	0.00	0.01

After solidification, the cast samples were polished with abrasive paper up to 1,200 followed by micro-polishing using a monocrystal diamond suspension (0.5 μm). Optical microscopy was carried out to characterize the microstructure of the alloys coupled with a Clemex image analysis software in order to determine the primary particle size and the solid fraction.

Macro-hardness measurements were carried out on each of the as-cast samples using a Mitutoyo ATK-600 hardness machine with the Rockwell *F* method (60 kg load and 1/16″ steel ball). The results of the average of six measurements were then converted to the standard Vickers hardness (10 kg load).

Results and discussion

Phase diagram predictions

Figure 1 shows the calculated phase diagram of the binary Al–Si alloy system. The dashed line at 17% Si indicates that the temperature of formation of primary Si and that of the binary eutectic reaction occur at 645.8 and 577.4 °C, respectively. The calculations confirm that the Si starts to precipitate as a primary phase from the liquid phase at 645.8 °C and continues to precipitate and grow below this temperature up to 577.4 °C, with a maximum solid fraction of 5.4%. At this point, which is also called "knee" point (Fig. 2), both eutectic α-Al and Si start to form isothermally and the remaining liquid solidifies at this temperature.

Figure 3 shows the isopleth diagram for the ternary Al–17%Si–Mg system with a variation of Mg content up to 10% Mg. It can be observed that the Mg_2Si phase appears in the diagram even at low Mg contents due to the solvus line. However, the temperature range of the formation of Mg_2Si intermetallic particles varies with Mg content during the solidification interval as shown by the line marked with star symbols in Fig. 3. This line is also called the zero phase fraction (ZPF) line of Mg_2Si.

The solvus line which corresponds to the initial region of the ZPF line of Mg_2Si indicates that the maximum solubility of Mg in α-Al solid solution is 0.54% Mg at 557.4 °C. The liquid and solid phase fractions of each constituent during the solidification interval and in the solid state of an alloy with a composition of Al–17%Si–0.3%Mg

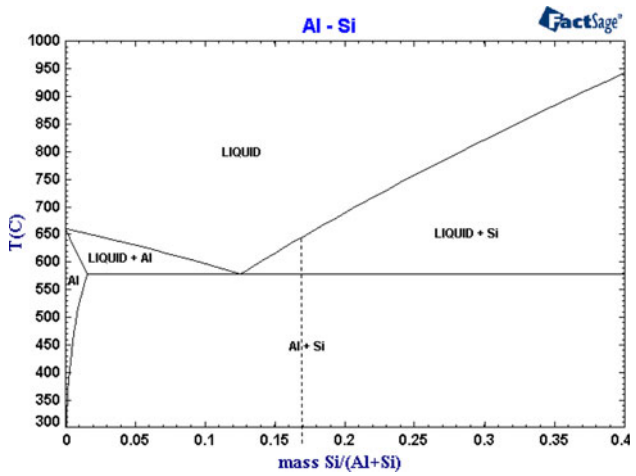

Fig. 1 Calculated binary Al–Si phase diagram. The *dashed line* represents the composition at 17% Si calculated by FactSage

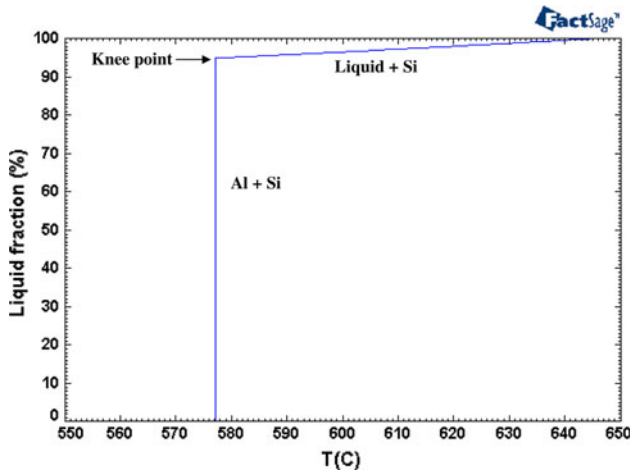

Fig. 2 The liquid fractions versus temperature for the basic Al–17Si% alloy for equilibrium condition

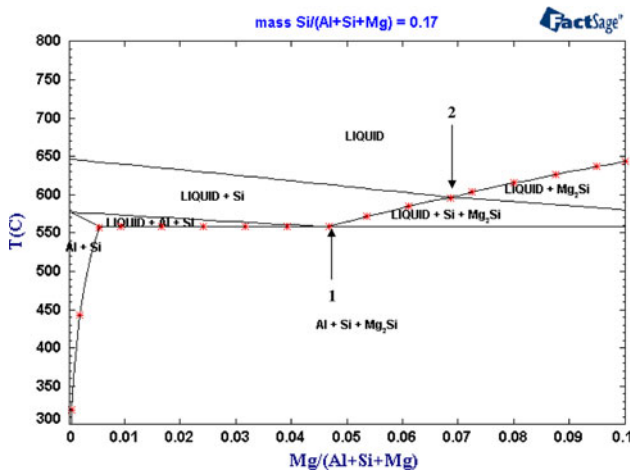

Fig. 3 Isopleth diagram for the ternary Al–17%Si–Mg system with the variation of up to 10% Mg

are shown in Fig. 4a. The precipitation of Mg_2Si particles starts at 489.3 °C according to the solvus line by the precipitation of Mg from α-Al solid solution, reacting with Si to form Mg_2Si particles as shown in Fig. 4b.

Two specific compositions, at 4.6 and 6.8% Mg, are indicated by arrows (points 1 and 2) on ZPF line of Mg_2Si. With Mg contents between 0.54 and 4.6%, solid Mg_2Si is formed near the end of the solidification and at the isothermal temperature of 557.4 °C where the last liquid

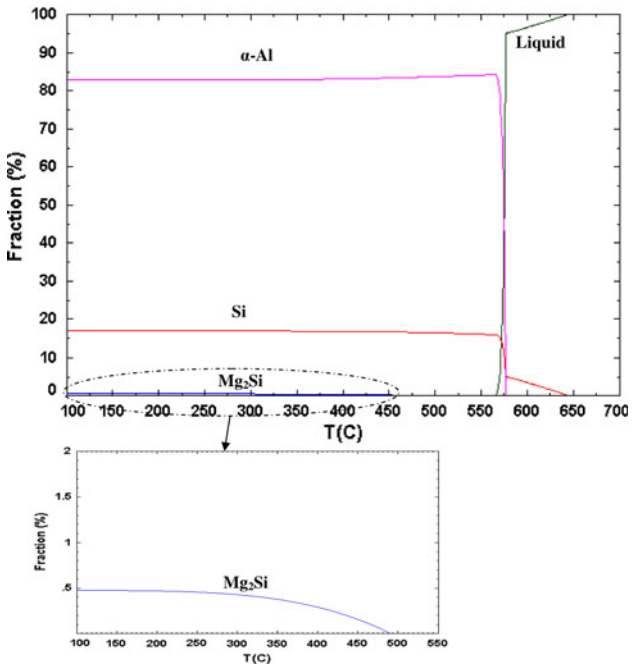

Fig. 4 The liquid and solid phase fractions of each constituent during the solidification interval of the alloy with composition of Al–17%Si–0.3%Mg. The inserted graph shows the Mg_2Si fraction line (*oval zone*) at high solid fraction

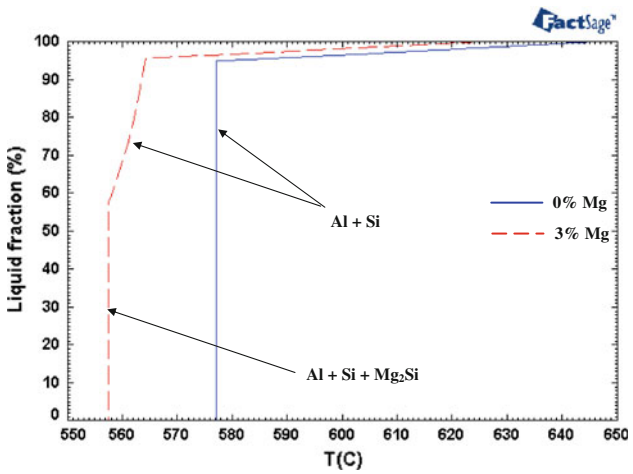

Fig. 5 Comparing the liquid fraction line for Al–17%Si alloy without and with 3% Mg addition

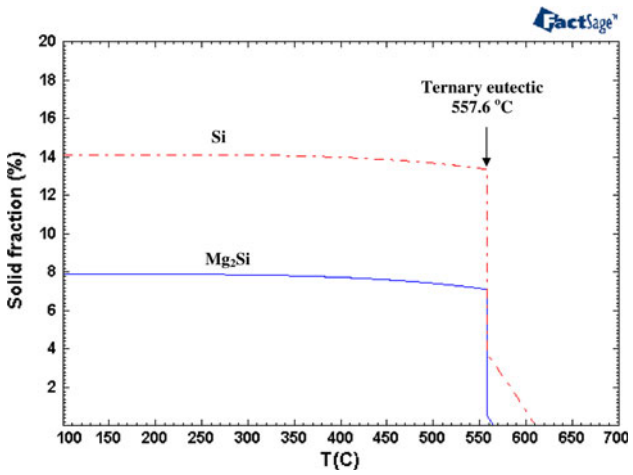

Fig. 6 The solid phase fraction lines of Si and Mg_2Si particles during the solidification interval of the alloy with composition of Al–17%Si–5%Mg

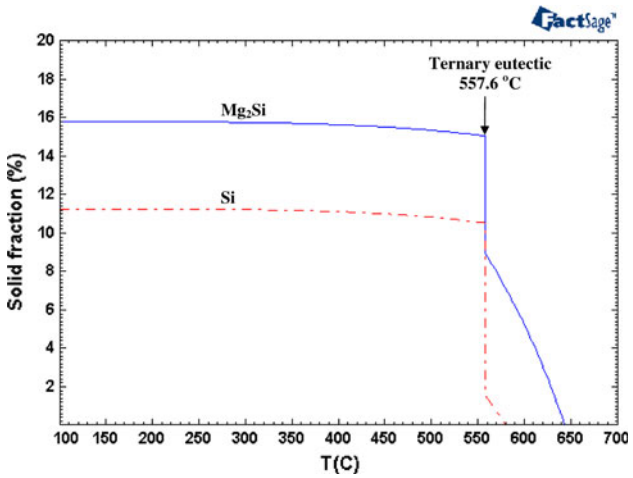

Fig. 7 The solid phase fraction lines of Si and Mg_2Si particles during the solidification interval of the alloy with composition of Al–17%Si–10%Mg

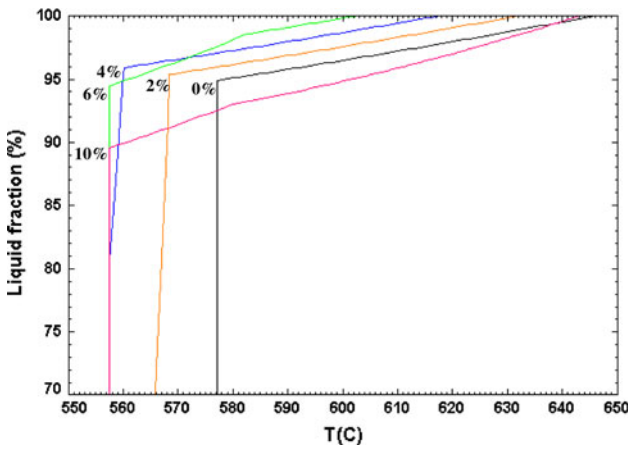

Fig. 8 Liquid fraction versus temperature curves of the basic Al–17%Si alloy and the alloys with addition of 2, 4, 6, and 10% Mg

solidifies to form solid Al, Si, and Mg_2Si according to the ternary eutectic reaction of Liq. → Al + Si + Mg_2Si. The addition of more than 0.54% Mg into the Al–17%Si alloy (base alloy) shifts the last isothermal eutectic reaction from the binary at 577.4 °C to the ternary reaction at 557.4 °C. Consequently, the binary eutectic reaction occurs isothermally for the base alloy followed by the precipitation of primary Si whereas, with the addition of more than 0.54% Mg, the binary eutectic microstructure is formed in a range of temperature before reaching the ternary eutectic reaction. This is shown in Fig. 5 which compares the liquid

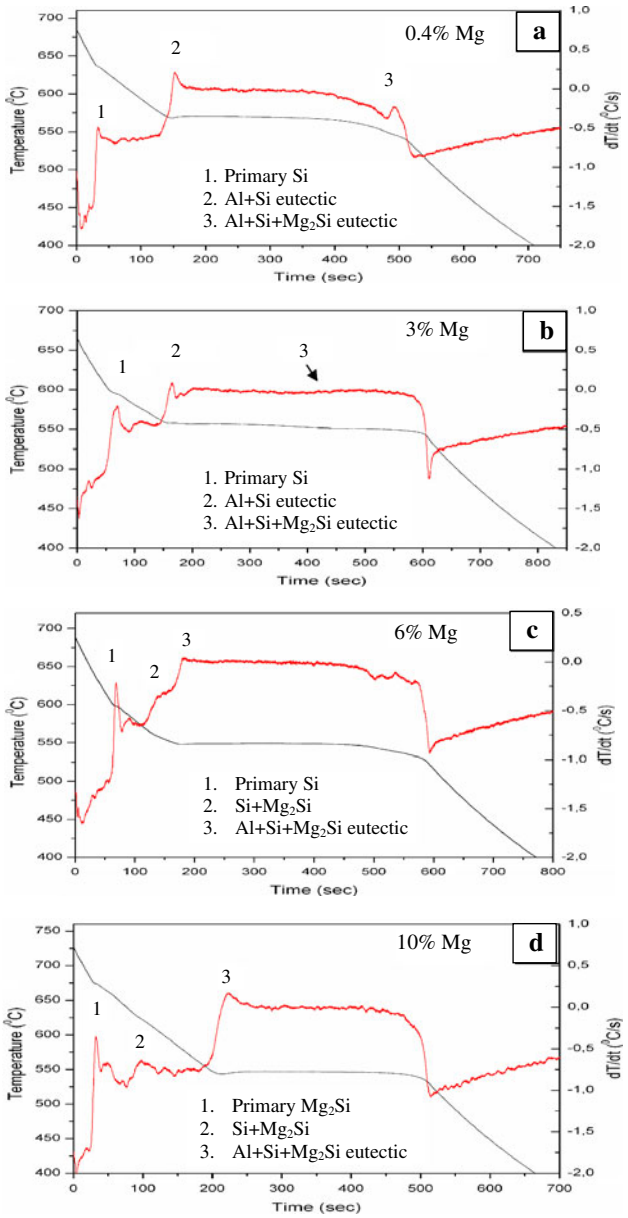

Fig. 9 The measured cooling curves and its first derivative during the solidification interval of the as-cast samples for the base binary alloy and the alloys with the addition of 0.4% Mg, 3% Mg, 6% Mg, and 10% Mg

fraction for the binary Al–17%Si with that of an Al–17%Si–3%Mg alloy during their respective solidification intervals.

It is anticipated that the eutectic network of the matrix for high Mg content alloys would result in a finer microstructure due to the increase of the number of the active sites for eutectic nucleation, which increases with decreasing temperature. Wear test studies have shown that the fine-eutectic matrix, particularly eutectic silicon in hyper-eutectic alloys, can resist wear more effectively than the matrix with a coarse microstructure [19]. Eutectic Mg_2Si in the form of Chinese script morphology [20] is also present in the eutectic network of high Mg content alloys and contributes to increased overall hardness. The authors have investigated the wear behavior of A390 hyper-eutectic Al–Si (Al–17%Si–4.5%Cu–0.5%Mg) alloy with the addition of 6 and 10% Mg and have observed the effect of the changing eutectic morphology of the matrix on the improvement of wear behavior of the alloy with high Mg content [17].

For alloys with Mg contents between 4.6 and 6.8% (between points 1 and 2 in Fig. 3), the Mg_2Si particles are formed as a result of both the binary and the ternary reactions. This implies that the intermetallic Mg_2Si particles are first formed along with the primary silicon particles followed by the precipitation of eutectic Mg_2Si in the ternary eutectic reaction. The solid phase fractions of Si and Mg_2Si formed during the solidification of Al–17%Si–5%Mg down to the ternary eutectic point at 557.6 °C and after the eutectic reaction are shown in Fig. 6.

Figure 6 indicates that both Si and Mg_2Si particles are solidified as pro-eutectic and as eutectic phases before and after the isothermal ternary eutectic reaction ($T = 557.6$ °C). However, the primary phase still consists of Si and Mg_2Si starts to form along side the Si particles only at 564.2 °C.

The calculated isopleth diagram shown in Fig. 3 indicates that the alloy with the lowest liquidus temperature of 595.1 °C is formed at 6.8% Mg. This liquidus temperature is about 50 °C lower than that of the base binary Al–17%Si alloy. Therefore, this composition presents the smallest range of the solidification interval that can be obtained for the alloys in this study.

Above 6.8% Mg, the Mg_2Si particles solidify as a primary phase as well as during the binary and ternary eutectic reactions over the whole solidification interval. This implies that the formation range of Mg_2Si intermetallic particles can be significantly increased with the addition of Mg. Figure 7 shows the case for 10% Mg addition. Above 6.8% Mg, the liquidus temperature increases again and the liquidus line corresponds to the final portion of the ZPF line of Mg_2Si as shown in Fig. 3.

Figure 8 compares the liquid fraction versus temperature curves of Al–17%Si alloys with contents of 0, 2, 4, 6, and 10% Mg. The figures shows that the start of the eutectic formation temperature of the matrix network (knee point) significantly decreases up to 4% Mg and then becomes almost constant for 6 and 10% Mg.

Thermal analysis

The measured cooling curves and their first derivatives during the solidification of the as-cast samples for the alloys with the addition of 0.4% Mg, 3% Mg, 6% Mg, and 10% Mg are shown in Fig. 9a–d. The main solidification reactions of these alloys are indicated for each composition. The measured reaction temperatures presented on the cooling curves are consistent with the results computed by the FactSage in predicting the changes in reaction temperatures, such as the liquidus and the start of the eutectic formation reaction of the matrix network, as indicating by the two critical points at 4.6 and 6.8% Mg shown in Fig. 10. The cooling curves show that the liquidus temperature decreases with the addition of Mg up to 6% and then increases again with further addition of Mg as

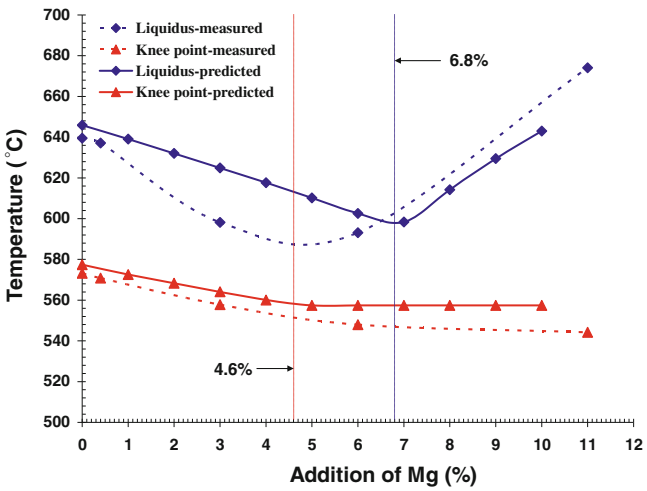

Fig. 10 Comparison of the measured reaction temperatures such as liquidus and the start of the eutectic formation reaction of the matrix network (knee point) temperatures on the cooling curves with the graphs computed by the FactSage according to the two critical points at 4.6 and 6.8%

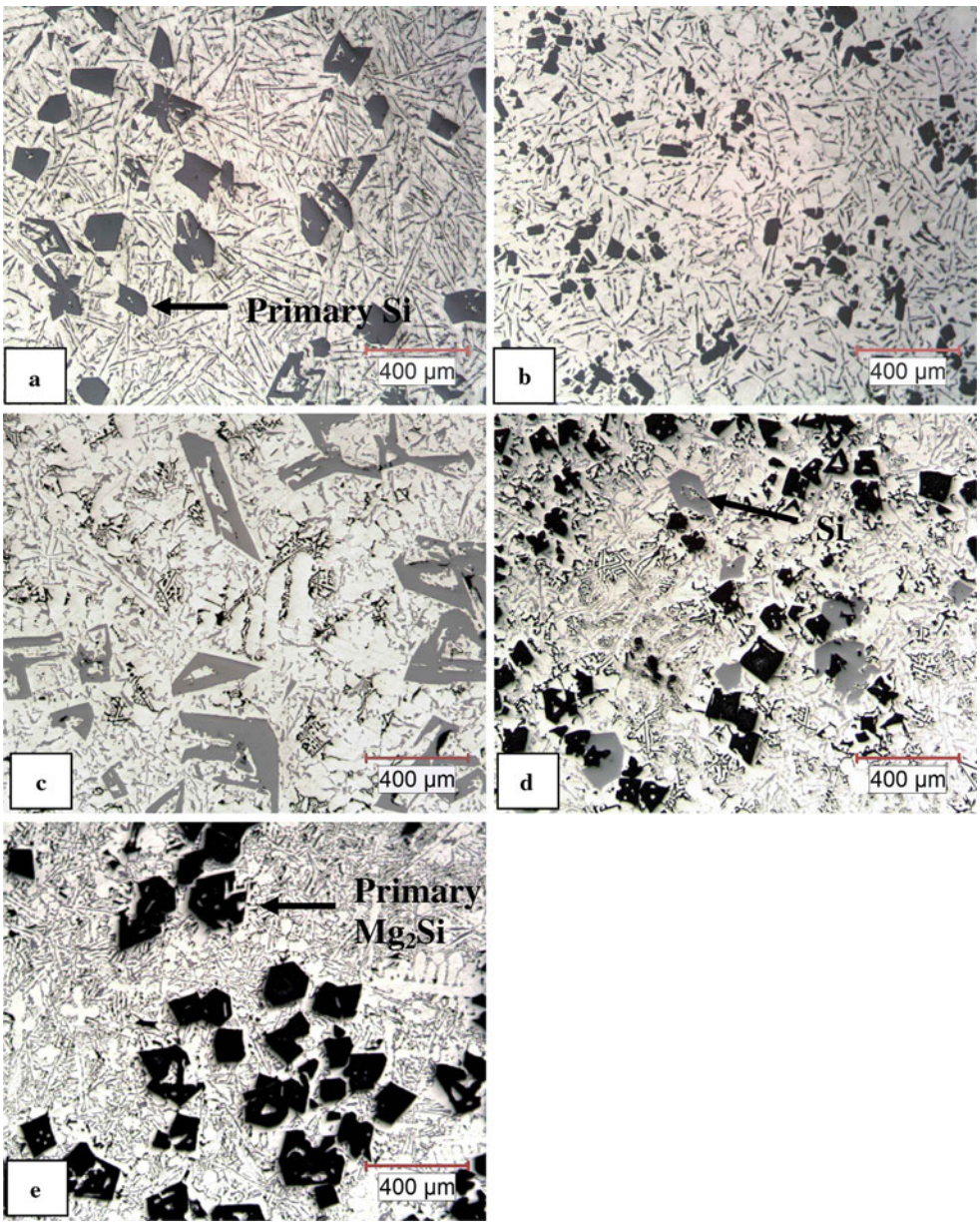

Fig. 11 The optical microstructure of the alloys in as-cast condition (**a**) Al–17%Si base alloy and the alloys with the addition of (**b**) 0.4% Mg, (**c**) 3% Mg, (**d**) 6% Mg, and (**e**) 10% Mg

Table 2 Comparison of the mean particle size of the primary phases as well as their solid fractions for the conventionally cast alloy samples

	Si		Mg_2Si	
	Mean particle size (μm)	Solid fraction (%)	Mean particle size (μm)	Solid fraction (%)
Base alloy (0% Mg)	93.6	8.8	–	–
0.4% Mg	49.2	7.9	–	–
3% Mg	131.4	12.1	–	–
6% Mg	110.1	6.7	65.1	7.3
10% Mg	–	–	98.5	18.6

predicted by the FactSage simulation. A minimum liquidus temperature at 6.8% Mg (second critical point) is followed by an increase of the liquidus temperature with further addition of Mg. It should be noted that the solidification of cast samples is always somewhat different from the equilibrium condition predicted by the FactSage simulation. For the addition of 0.4% Mg, the ternary eutectic reaction (Liq. $\rightarrow$ Al + Si + Mg_2Si) appears near the end of the solidification due to a non-equilibrium condition. The liquidus temperatures obtained from the cooling curves can also be lower than the predicated values due to the undercooling. This was clearly observed for the alloy with the

addition of 3% Mg. The reduction of the knee point temperature implies that the eutectic reaction of the matrix shifts from the binary to the ternary eutectic reaction with the addition of Mg, which is the main contributing factor in the changes of the morphology of the eutectic phases in the matrix network.

Microstructural observation

Evolution of primary phases

Figure 11 shows an optical images of the microstructure of the alloys for the as-cast condition. The base alloy, Fig. 11a, contains large polygonal or star like primary silicon particles dispersed in a binary eutectic network of Al + Si in the matrix. With the addition of 0.4% Mg to the binary alloy, the size of the primary silicon decreases significantly as shown in Fig. 11b. At 3% Mg, Fig. 11c, the size of the primary silicon increases again to a size larger than the base alloy. The anomalous increase in the size of primary silicon particles may have resulted in a reduced number of primary Si particles which increase the particle size of primary silicon. Figure 11d shows the microstructure of the alloy with the addition of 6% Mg. It can be seen that the Mg_2Si particles generally appear together with the primary silicon particles with a common interface and

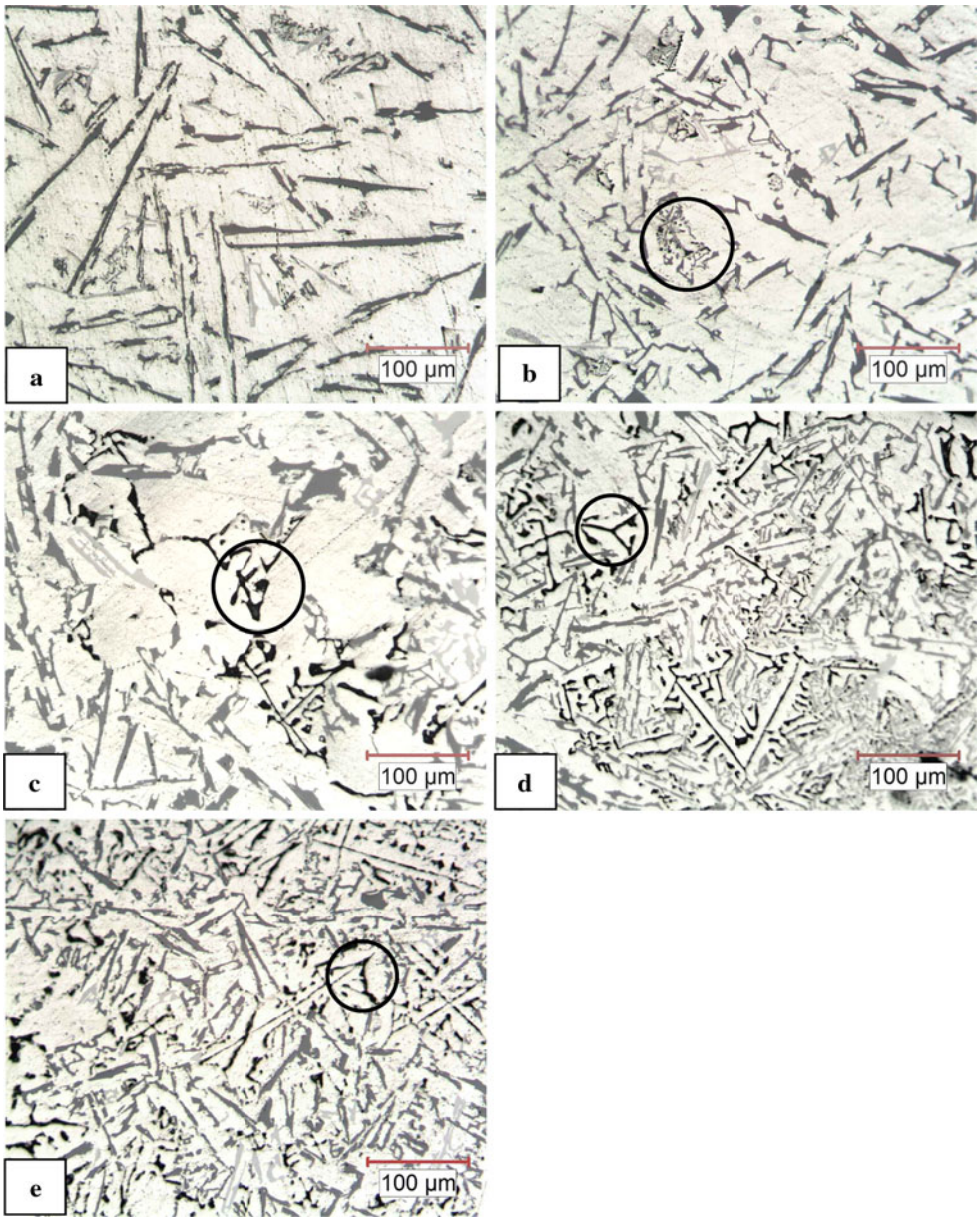

Fig. 12 The optical eutectic matrix microstructure of the alloys in as-cast condition. (**a**) Al–17%Si base alloy and the alloys with the addition of (**b**) 0.4% Mg, (**c**) 3% Mg, (**d**) 6% Mg, and (**e**) 10% Mg. The *circled zones* present the eutectic Mg_2Si

again the particle size of primary silicon is larger than that found in the binary alloy. Therefore, the formation of Mg_2Si particles affects the size of primary silicon particles. The morphology of the Mg_2Si particles also varies from dendritic to polygonal. At 10% Mg (Fig. 11e), almost all of the primary silicon particles are replaced by primary Mg_2Si particles. Table 2 compares the mean particle size of the primary phases as well as their solid fractions for the case of as-cast samples. The primary silicon particles are smallest at 0.4% and largest at 3% Mg. The mean particle size of the Mg_2Si intermetallic phase tends to increase with the addition of Mg >6%. The total solid fraction of primary phases increases from 8.8 to 18.6% for the alloy with 10% Mg.

Evolution of the eutectic phases

Figure 12a–e shows the microstructure of the eutectic network for the alloys in the as-cast condition for each composition. The morphology and size of the eutectic silicon particles change dramatically with the addition of Mg from individual and long-platelet shapes to a fine and compact form with a Chinese script like morphology. The interparticle space (λ) of the eutectic Si decreased from 9.2 to 4.8 μm indicating a more compact eutectic network for the matrix of the 10% Mg alloys as compared to the base alloy. Eutectic Mg_2Si particles are observed in the eutectic network of the alloys with Chinese script morphology as shown by circled zones indicated in Fig. 12. The presence of the eutectic Mg_2Si particles was also observed even for the lowest addition of 0.4% Mg (Fig. 12b) due to the occurrence of the ternary eutectic reaction at non-equilibrium solidification, as shown in Fig. 9a.

The values of the average hardness obtained from the as-cast samples are compared in Fig. 13 with the samples of A390 hyper-eutectic Al–Si (Al–17%Si–4.5%Cu–0.5%Mg) alloy with the addition of 6 and 10% Mg [17]. The A390 alloys were cast in a standard permanent mold (rapid cooling) while the samples in the present work were solidified at a slow-cooling rate as was explained before. The value of the hardness of the binary alloy increases significantly with increasing up to 6% Mg content even though the hardness of the Mg_2Si particles measured by micro-hardness machine was found to be at least half of value of the primary silicon particles (Si = 1148 HV, Mg_2Si = 505 HV). The hardness then gradually increases for Mg content >6%. Therefore, the changes that occur in the eutectic phases as well as the increase of the total solid fraction of primary phases are the main contributing factors in the increase of the overall hardness with increased addition of Mg.

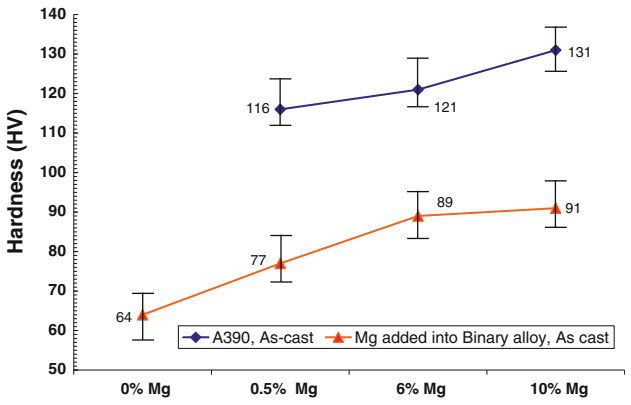

Fig. 13 Comparison of the effect of addition of Mg on the average hardness of the binary Al–17%Si samples solidified in static air and A390 (Al–17%Si–4.5%Cu–0.5%Mg) alloy in as cast in permanent mold and after T6 heat-treated conditions

Conclusions

The reaction temperature during the solidification interval of the binary Al–17%Si alloy was calculated using the FactSage® software with the addition of Mg contents up to 10 wt%. The maximum solubility of Mg in α-Al solid solution was determined to be 0.54% Mg at 557.4 °C and resulted in formation of Mg_2Si intermetallic particles in the solid state according to the solvus line. At higher Mg content, the calculations have identified two critical compositions at 4.6 and 6.8% Mg where the liquidus, the binary reaction as well as the temperature range for the formation of Mg_2Si particles is changed during solidification of binary alloy with the addition of Mg.

The predicted reaction temperatures show good consistency with the measured cooling curves using two K-type thermocouples during solidification studies of the binary alloy with different Mg additions. The considerable reduction of the start of the eutectic formation temperature (also called knee point) with the different addition of Mg up to 4.6% was confirmed. This reduction in the eutectic formation temperature of the matrix is due to the change of the eutectic formation reaction from the binary (Liq. → Al + Si) to the ternary (Liq. → Al + Si + Mg_2Si). This change affects the size and morphology of the eutectic silicon phase in the matrix.

The cast microstructure of the base alloy (0% Mg) and alloys with addition of 0.4, 3, 6, and 10% (wt%) Mg conventionally cast from liquid state at temperatures between 700 and 710 °C into a preheated thin shell stainless steel crucible demonstrated that the morphology of the eutectic silicon changes with the addition of Mg from individual and long platelet form to fine and compact form with a Chinese script morphology, similar to the eutectic Mg_2Si phase. This change in morphology is the main factor in the decrease of the eutectic reaction temperature with the

addition of Mg. This change in morphology of the eutectic matrix ultimately resulted in the increase of the overall hardness of the high Mg alloys even though the hardness of the primary Mg_2Si particles is lower than that of the primary silicon particles.

A modification of both primary and eutectic silicon particles size was only observed for the alloy with the lowest Mg content (0.3% Mg) when compared to the base binary Al–17%Si alloy. This indicates that Mg can act as a modifier of silicon particles at this level of concentration. More studies needs to be carried out to determine the mechanism of modification and the determination of the optimum value of Mg for the greatest modification.

Acknowledgements The authors gratefully acknowledge the financial support from the Natural Sciences and Engineering Research Council of Canada (NSERC). The authors also thank Mr. Mehand Tebib of Université du Québec à Chicoutimi for the help in the thermal analysis.

References

1. Timmermans G, Froyen L (1999) Wear 230:105
2. Rohatgi PK, Asthana R, Das S (1986) Int Met Rev 31:115
3. Gupta M, Ling S (1999) J Alloys Compd 287:284
4. Midson S, Keist J, Svare J (2002) In: SAE 2002 world congress Detroit, MI, March 4–7, 2002-01-394
5. Kyffin WJ, Rainforth WM, Jones H (2001) Mater Sci Technol 17:901
6. Zhang H, Duan H, Shao G, Xu L (2008) Rare Met 27:59
7. Jiang QC, Xu CL, Lu M, Wang HY (2005) Mater Lett 59:624
8. Lashkari O, Ajersch F, Charette A, Chen X-G (2008) Mater Sci Eng A 492:377
9. Kapranos P, Kirkwood DH, Atkinson HV, Rheinlander JT, Bentzen JJ, Toft PT, Debel CP, Laslaz G, Maenner L, Blais S, Rodriguez-Ibabe JM, Lasa L, Giordano P, Chiarmetta G, Giese A (2003) J Mater Process Technol 135:271
10. Wang F, Ma Y, Zhang Z, Cui X, Jin Y (2004) Wear 256:342
11. Birol Y (2008) J Mater Process Technol 207:200
12. Hekmat-Ardakan A, Ajersch F (2010) J Mater Process Technol 210(5):767
13. Hekmat-Ardakan A, Ajersch F (2010) J Mater Charact 61:778
14. Mandal A, Makhlouf MM (2010) Int J Cast Met Res 23:303
15. Zhang J, Fan Z, Wang YQ, Zhou BL (2000) Mater Sci Eng A 281:104
16. Li SP, Zhao SX, Pan MX, Zhao DQ, Chen XC, Barabash OM (2001) J Mater Sci 36:1569. doi:10.1023/A:1017525520066
17. Hekmat-Ardakan A, Liu X, Ajersch F, Chen X-G (2010) Wear 269(9–10):684
18. Bale CW, Pelton AD. FactSage 5.4.1. C.R.C.T (Centre of Research for Computational Thermochemistry), École Polytechnique de Montréal. http://www.crct.polymtl.ca
19. Birol Y, Birol F (2008) Wear 265:1902
20. Qin QD, Zhao YG, Cong PJ, Liang YH, Zhou W (2006) Mater Sci Eng A 418:193